Available online at www.sciencedirect.com
SCIENCE DIRECT®
PERGAMON
Polyhedron 22 (2003) 1167–1181
POLYHEDRON
www.elsevier.com/locate/poly

Synthesis, crystal structure and characterisation of aquamagnesium phthalocyanine—MgPc(H_2O). The origin of an intense near-IR absorption of magnesium phthalocyanine known as 'X-phase'

Jan Janczak [a,b,*], Ynara Marina Idemori [a]

[a] *Instituto de Ciências Exatas, Departamento de Química, Universidade Federal de Minas Gerais, CEP 31270-901, Belo Horizonte, MG, Brazil*
[b] *Institute of Low Temperature and Structure Research, Polish Academy of Sciences, P.O. Box 1410, 50-950 Wroclaw, Poland*

Received 14 October 2002; accepted 19 December 2002

Abstract

The crystals of a triclinic modification of MgPc(H_2O) were obtained by dissolving MgPc in benzonitrile with a small amount of water and slow recrystallization at about 80 °C. In the crystal there are two independent MgPc(H_2O) molecules in the asymmetric unit. The independent molecules are very similar, the 4+1 coordinated central magnesium atom is significantly displaced from the N_4-isoindole plane of the distorted Pc rings (~ 0.45 Å) toward the oxygen atom of coordinated water molecules. The geometry of the MgPc(H_2O) molecule in the crystal (C_1-symmetry) is compared with the ab initio full-optimised geometry (C_{4v}) that corresponds to the conformation of the molecule in solution. In contrast to the monoclinic modification of MgPc(H_2O), which is not near-IR active, this triclinic modification shows an intense broad absorption band in this spectral region that is very similar to that observed in the solid state spectrum of β-MgPc. The near-IR absorption is characteristic only for the solid state samples since the spectra of MgPc(H_2O) and β-MgPc in pyridine solution are similar and show only one intense Q band with characteristic splitting due to the vibronic coupling in the excited state. The intense absorption band observed in the spectrum of solid state of MgPc(H_2O) as well as in the spectrum of β-MgPc originates from the arrangement of the molecules in dimers with strong π–π interactions between the distorted Pc macrorings. The molecular distortion (reduction in the symmetry $C_{4v} \rightarrow C_1$) lifts the double degeneracy of the excited state.

Keywords: Recrystallization; MgPc(H_2O); Photodynamic

1. Introduction

Considerable interest in magnesium phthalocyanine, MgPc where Pc = $C_{32}H_{16}N_8$, and its 4+1 and 4+2 coordinated complexes, MgPcL and MgPcL_2 (where L is a N or O donor ligand), arises from their similarity and relationship to chlorophyll and they can be used as its synthetic model [1,2]. On the other hand their electrochemical properties make them useful in several fields where phthalocyanines find application. Due to their intense blue colour, they are used as pigments in display devices, for laser printers, for optical disks and as photochemical redox agents in solar conversion [3–10]. A number of magnesium phthalocyaninato complexes, especially the sulfonated and alkyl-substituted derivatives, similar to other closed shell metallophthalocyaninato complexes such as Zn(II), In(III) or Ga(III), are used in medicine as photosensitisers for photodynamic cancer therapy due to their possibility to generate oxygen in the singlet state and their non-toxicity [11–17]. During photodynamic therapy with phthalocyanine as a photosensitiser, it is excited to its singlet state and then transfers the energy to ground-state triplet oxygen, O_2 ($^3\Sigma_g$) forming the excited state singlet oxygen, O_2 ($^1\Delta_g$).

Magnesium phthalocyanine (MgPc) similar to other metal(II) phthalocyaninato complexes (M(II)Pc) crystallises in two crystallographic modifications—α and β.

* Corresponding author. Tel.: +48-71-343-5021; fax: +48-71-441-029.
E-mail addresses: jjanek@dedalus.lcc.ufmg.br, janczak@int.pan.wroc.pl (J. Janczak).

0277-5387/03/$ - see front matter
doi:10.1016/S0277-5387(03)00110-4

However, the single crystal structure has been determined only for the β modification [18]. For the same metal, up until now there is no example of the single crystal structure determination for both α and β forms; only the α modification for PtPc or PdPc or only the β modification for several transition metals such as Mn, Fe, Co, Ni, Cu and Zn were determined on single crystals. The metal-free phthalocyanine, H_2Pc, is the unique example for which the single crystal structures of both α and β modifications have been determined [19–21]. Additionally, it has been stated that the crystals of MgPc are unstable in ambient atmosphere and absorb O_2 and/or N_2 forming complexes with the compositions of $(MgPc)_2O_2$ and $(MgPc)_2N_2$ [18,22]. The formation of $(MgPc)_2O_2$ as well as $(MgPc)_2N_2$ is reversible and strongly depends on the temperature [18]. The instability of the β-MgPc crystals as well as the unusual and different behaviour of MgPc in relation to the other β M(II)Pc complexes such as CuPc, FePc, CoPc, MnPc are still not clear. Quite recently the single crystal investigations of MgPc [18] enabled us to explain these differences. The crystal structure analysis shows that the magnesium atom is, in contrast to other M(II)Pc complexes, significantly displaced from the N_4-isoindole plane (~ 0.5 Å) although the ab initio molecular orbital calculation predicts its planarity [23–25]. In the crystal the interaction of the positively charged magnesium atom ($\sim +0.5$ charged as the MO calculation shows) with the *N*-azamethine atom of the neighbouring the MgPc molecule is the reason for the displacement of Mg from the N_4-isoindole plane toward the *N*-azamethine atom, so the Mg accommodates the 4+1 coordination.

The most interesting and characteristic properties are possessed by the magnesium phthalocyanine, which is called in the literature 'X-phase', since it exhibits an intense band absorption in the near-IR spectral region [26–30]. The origin and the nature of this near-IR absorption up to now are still not clear. Endo et al. [31] suggested that the near-IR absorption arises from exciton coupling effects, i.e., the interactions between the transition dipoles and assigned to the 'X-phase' composition of $MgPc(H_2O)_2$. They have analysed the average spectrum obtained by the superposition of the two polarised reflection spectra for a single crystal of $MgPc(H_2O)_2 \cdot (NMP)_2$, where NMP = *N*-methyl-2-pyrrolidone [32] and stated that this average spectrum slightly resembles the spectrum of the 'X-phase' and therefore they assigned $MgPc(H_2O)_2$ as a composition of the 'X-phase'. However, the intense near-IR absorption is observed on the solid state sample of the 'X-phase', i.e., as an evaporated thin solid film, while in solution the spectrum is similar to the spectrum of other M(II)Pc complexes and shows two characteristic Q- and B-Soret bands typical for the phthalocyaninato ring. On the other hand the temperature used for the evaporated formation of the thin solid film of the 'X-phase'' for the UV–vis experiment is much higher than allowed by the thermal stability of the $MgPc(H_2O)_2$ complex assigned to the ''X-phase' by Endo et al. [31]. For this reason we think that the composition of the 'X-phase' is not $MgPc(H_2O)_2$ and the origin of the intense near-IR absorption is not from the interaction of the MgPc molecule with two water molecules as was suggested in the literature [29,30].

Herein we investigate the solid state structure of the triclinic modification of aquamagnesium phthalocyanine, $MgPc(H_2O)$. The geometry of the $MgPc(H_2O)$ molecule is compared with the monoclinic modification, that was described recently [33]. The X-ray geometry of $MgPc(H_2O)$ of both modifications is compared with the gas-phase geometry obtained by ab initio molecular orbital calculations. Additionally, a new examination and explanation of the intense near-IR absorption band in the spectrum of the 'X-phase' of magnesium phthalocyanine are proposed.

2. Experimental

2.1. Preparation

The MgPc used for the synthesis of $MgPc(H_2O)$ was obtained by the procedure described previously [18]. The single crystals of $MgPc(H_2O)$ suitable for the X-ray analysis were obtained by the following procedure. 0.54 g (0.1 mmol) MgPc was added to a mixture of 100 ml benzonitrile and 4 ml H_2O under reflux in an inert (Ar) atmosphere over about 6 h. Next the reaction was kept at 120 °C for 2 days, and then slowly cooled with a temperature gradient of 0.5 °C h^{-1}. The first crystal appeared at the temperature ~ 80 °C. At this temperature the crystallisation process was continued for 1 month, and then the reaction mixture was cooled quickly to room temperature. The obtained crystals in suspension were filtered, washed with acetone and dried. The elemental analysis of the product (~ 0.48 g, 85.7%) was performed on a dispersive energy spectrometer and yielded: Mg, 4.32; C, 69.38; N, 20.12; H, 3.24 and O, 2.94%. Calc. for $C_{32}H_{16}N_8MgH_2O$: Mg, 4.38; C, 69.27; N, 20.19; H, 3.28 and O, 2.88%.

2.2. Thermal measurement

Thermal analysis was carried out on a Lines L81 thermobalance apparatus with Pt-crucibles. Powdered Al_2O_3 has been used as reference. The measurement has been performed under static air atmosphere on heating from room temperature to 300 °C at the heating rate of 2 °C min^{-1}.

2.3. X-ray data collection

A violet single crystal of $MgPc(H_2O)$ having edges of 0.25 mm × 0.22 mm × 0.16 mm was measured on an Enraf-Nonius Kappa-CCD diffractometer with graphite monochromatized Mo Kα ($\lambda = 0.71073$ Å) radiation at 100 K (nitrogen low temperature attachment, Oxford Cryosystem). The final unit cell parameters were refined by least-squares methods on the basis of all reflections. 47397 (11221 independent, $R_{int} = 0.0406$) reflections were measured up to 55° in 2ϑ covering over 99% of the Ewald sphere. Data collections were made using the COLLECT program [34], integration and scaling of the reflections were performed with the HKL Denzo-Scalepack system of programs [35]. Absorption corrections were carried out using the multi-scan method [36].

The structure was solved by direct methods using the SHELXS-97 program [37]. Fourier maps were calculated from $E \geqslant 1.8$ that gave the positions of the magnesium, oxygen and most of the nitrogen and carbon atoms of the phthalocyaninato rings. The remaining atoms were located from the difference Fourier synthesis. The hydrogen atoms of the phenyl rings were located from the $\Delta\rho$ maps and in the final refinement they were refined with the riding model [37]. The H atoms of the water molecules were set as isotropic with thermal parameters 50% greater than the equivalent isotropic displacement parameter of the oxygen atom. The final differences Fourier map showed no peaks of chemical significance. The largest peaks on the final $\Delta\rho$ map were +0.367 and −0.287 e Å^{-3}. Scattering factors for neutral atoms and corrections for anomalous dispersion were as in SHELXS-97 [37]. Details of the data collection parameters, crystallographic data and final agreement parameters are collected in Table 1.

2.4. Spectroscopic measurements

The electronic absorption spectra were carried out at room temperature using a CARRY-VARIAN/5E UV–vis–NIR spectrometer. The solid state spectra of MgPc and $MgPc(H_2O)$ were recorded from thin film nujol mulls. The spectra in pyridine solution were performed in 0.5-cm quartz cells. IR (KBr pellet) and far-IR spectra (nujol mulls, polyethylene disks) were recorded at room temperature on a Bruker—IFS 113 V FT-IR spectrometer.

2.5. Theoretical calculations

Ab initio molecular orbital calculations were performed with the GAUSSIAN94 program package [38] at the Hartree-Fock level of theory. Full-optimisations were carried out with the 6-31G(d, p) basis set functions starting from the X-ray geometry. As a convergence criterion the threshold limits of 0.00025 and 0.0012 a.u. were applied for the maximum force and the displacement, respectively.

Table 1
Crystallographic data and final refinement parameters for $MgPc(H_2O)$

Chemical formula	$C_{32}H_{16}N_8Mg(H_2O)$
Molecular weight	554.85
Temperature (K)	100(2)
Crystal system	triclinic
Space group	$P\bar{1}$ (No. 2)
Unit cell dimensions	
a (Å)	12.9550(5)
b (Å)	13.2540(6)
c (Å)	16.0210(7)
α (°)	65.09(1)
β (°)	81.73(1)
γ (°)	83.62(3)
V (Å^3)	2465.12(18)
Z	4
D_{obs} (measured by flotation) (g cm^{-3})	1.488 (measured at room temperature)
D_{calc} (g cm^{-3})	1.495 (at 100 K)
Radiation, Mo Kα (Å)	0.71073
Absorption coefficient, μ (mm^{-1})	0.119
Refinement on F^2	
$R[F^2 > 2\sigma(F^2)]$ [a]	0.0488
$wR(F^2$ all reflections) [b]	0.0982
Goodness-of-fit, S	1.039
Residual electron density, $\Delta\rho_{max}$, $\Delta\rho_{min}$ (e Å^{-3})	+0.367, −0.287

[a] $R = \Sigma||F_o|-|F_c||/\Sigma F_o$.
[b] $wR = \{\Sigma[w(F_o^2-F_c^2)^2]/\Sigma wF_o^4\}^{1/2}$; $w^{-1} = [\sigma^2(F_o^2)+(0.0301P)^2+0.8806P]$, where $P = (F_o^2+2F_c^2)/3$.

3. Results and discussion

3.1. Synthesis and stability of $MgPc(H_2O)$

The crystals of a triclinic modification of $MgPc(H_2O)$ have been obtained during a prolonged crystallisation process from a solution of MgPc in benzonitrile/H_2O at about 80 °C, in contrast to the crystals of monoclinic modification, which were obtained from acetone solution at room temperature [33]. Although the MgPc:H_2O was used in a molar proportion greater than 1:1, the formed crystals contain only one water molecule per MgPc molecule, not two water molecules as suggested in the literature [31,32]. The crystals of $MgPc(H_2O)$ (triclinic modification) are stable at ambient atmosphere at room temperature. This is in contrast to the crystals of MgPc which rapidly polycrystallise, because the MgPc molecules interact with the air molecules, O_2 and N_2 (confirmed by two separate experiments in pure O_2 and in pure N_2), transforming into complexes with the compositions of $(MgPc)_2O_2$ and $(MgPc)_2N_2$ [22]. The behaviour of the crystals of MgPc, quite different to the other M(II)Pc complexes, is due to the significant

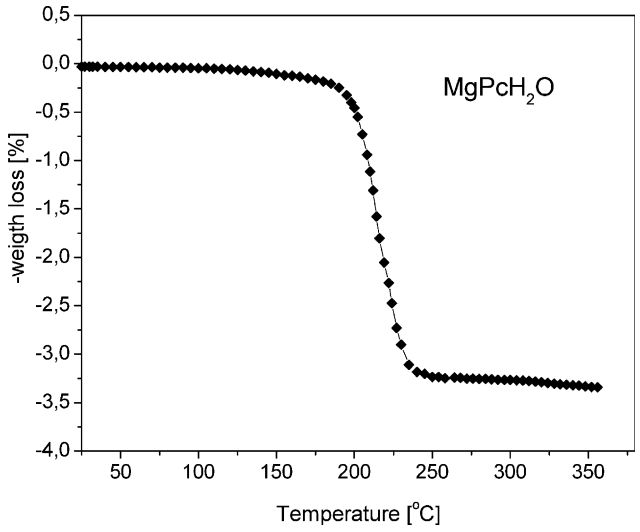

Fig. 1. Thermogram for the $MgPc(H_2O)$ complex. Heating rate 2 °C min^{-1}.

displacement (~0.5 Å) of the Mg atom from the phthalocyaninato(2-) ring, since the central Mg atom of a MgPc molecule with the effective positively charge of ~0.5 interacts with the *N*-azamethine atom of a neighbouring MgPc molecule [18]. This interaction leads to the formation of the dimer of magnesium phthalocyanine, $(MgPc)_2$, which is stabilised by 4+1 coordination of the central Mg atom. The existence of the dimers in the crystal of MgPc as subunits fully correlates with the composition of the complexes that are formed under ambient atmosphere [22].

As can be seen from the thermogram (Fig. 1) the complex of $MgPc(H_2O)$ is stable up to about 210 °C. Above this temperature the Mg–O bond in the $MgPc(H_2O)$ molecule breaks, giving MgPc in crystalline form, its powder diffraction pattern indicating the β-form. This is consistent with the results of our earlier studies of MgPc, which indicate that thermal treatment of MgPc samples above 200 °C yields always the β-modification of MgPc [22]. The crystals of $MgPc(H_2O)$ are well soluble in pyridine, DMF, DMSO and other N- and O-donor solvents as well as in high-boiling aromatic solvents like chloronaphthalene or quinoline. The relatively good solubility of $MgPc(H_2O)$ in pyridine is due to the interaction of pyridine molecules with the coordinated water molecule and formation of O–H···N(py) hydrogen bonds (Scheme 1). After several days from the solution in pyridine the crystals of $MgPc(H_2O) \times 2py$ appear [39]. In the crystal of $MgPc(H_2O) \times 2py$ both hydrogen atoms of coordinated water molecule are involved in hydrogen bonds with the pyridine molecules [40]. The crystals of $MgPc(H_2O)$ are insoluble in water. This can be explain on the basis of the molecular arrangement in the crystals; the hydrophilic part of the $MgPc(H_2O)$ complex is surrounded by hydrophobic phenyl rings of phthalocyaninato(2-) ligands due to formation of the dimeric structure—$[MgPc(H_2O)]_2$.

3.2. Description of the structure of $MgPc(H_2O)$

Refinement of the crystal structure of aquamagnesium phthalocyanine established that there are two independent $MgPc(H_2O)$ molecules in the asymmetric unit with very similar geometry (see Fig. 2(a) and (b)). In both molecules the magnesium atom is significantly displaced from the weighted-plane defined by the four *N*-isoindole atoms of the phthalocyaninato(2-) rings toward the oxygen atom of the water molecules. The displacement of the Mg atom from the N_4-isoindole

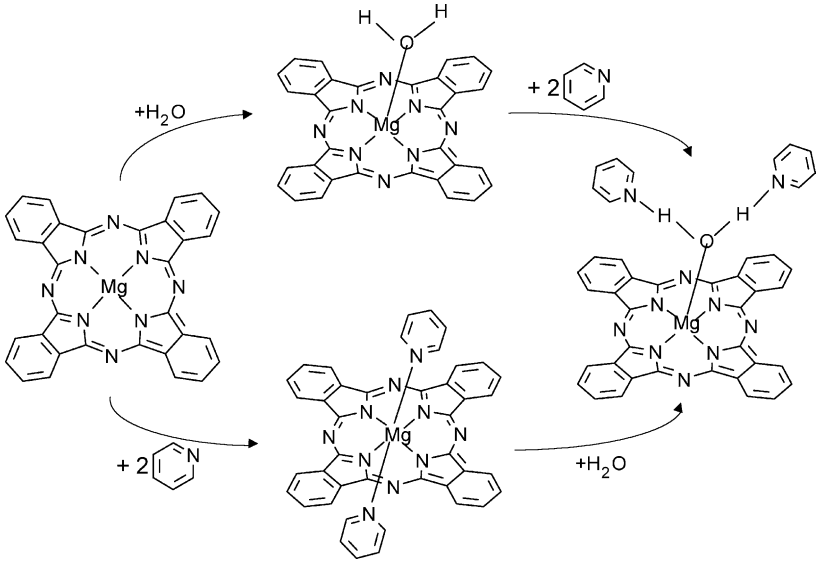

Scheme 1.

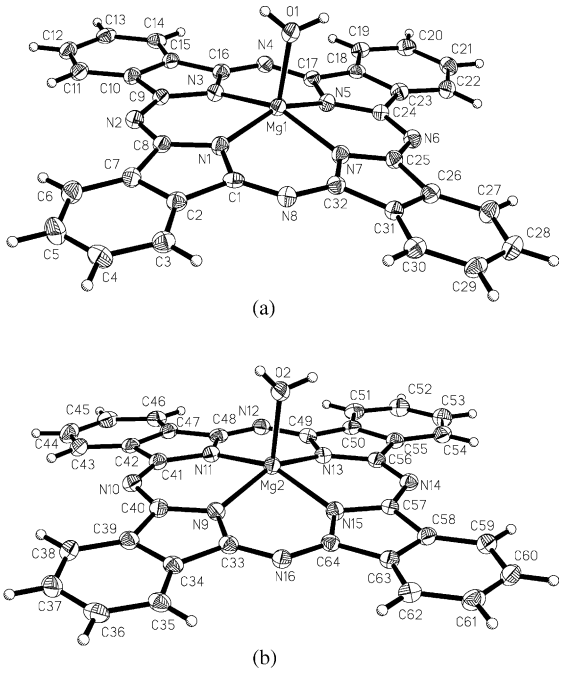

Fig. 2. Molecular structure of both independent MgPc(H_2O) molecules with labelling scheme, view of the molecule 1 (a) and molecule 2 (b). Displacement ellipsoids are shown at the 50% probability level. H atoms are shown as spheres with arbitrary radii.

plane is equal to 0.442(3) and 0.465(3) Å for Mg1 and Mg2, respectively. The displacement of the Mg atom from the N_4-plane is comparable to that observed in the monoclinic modification (0.47 Å), although the refinement parameters of the monoclinic form of MgPc(H_2O) are relatively high: $R = 10.6\%$ and $wR(F^2) = 20.9\%$ [33]. In the other two aquamagnesium phthalocyaninato(2-) complexes i.e., in MgPc(H_2O) × 2py [40] and [MgPc)H_2O)]$_2$ × 3py [41] the displacements of the Mg atoms from the N_4-isoindole plane are comparable. As can be seen from Table 3 the deviation of the central Mg atom from the N_4-plane in magnesium phthalocyaninato(2-) complexes is greater than in magnesium porphyrinato complexes [42–44] and in chlorophyll derivatives [45,46], which well correlate with the greater flexibility of the porphyrinato ring as well as the larger hole in relation to the phthalocyaninato ring. In all the above mentioned magnesium phthalocyaninato and porphyrinato complexes the central magnesium atom is coordinated by four N-pyrrole atoms and axially by the oxygen atom of a water molecule. This coordination of the Mg is quite similar to that found in chlorophyll. The 4+1 coordination number of the magnesium atom is also observed in the β form crystal of MgPc [18] due to the intermolecular interactions between the positively charge Mg atom of one MgPc molecule and the azamethine nitrogen atoms of a neighbouring MgPc molecule. The Mg···$N_{azamethine}$ intermolecular interactions lead to the comparable deviation of the Mg atom from the macrocyclic Pc ring as found in the aquamagnesium phthalocyaninato complexes. This Mg···$N_{azamethine}$ interaction in the crystal of MgPc is responsible for the non-planarity of the MgPc molecule and for the formation of the dimeric structure of MgPc [18]. The

Table 2
X-ray and optimised bond lengths (Å) for MgPc(H_2O)

	Molecule 1		Molecule 2	Opt. geometry HF/6-31G(d, p)
Mg1–O1	2.0076(14)	Mg2–O2	2.0357(14)	2.142
Mg1–N1	2.0380(15)	Mg2–N9	2.0468(15)	2.039
Mg1–N3	2.0419(14)	Mg2–N11	2.0455(15)	2.037
Mg1–N5	2.0477(15)	Mg2–N13	2.0396(15)	2.025
Mg1–N7	2.0488(15)	Mg2–N15	2.0470(15)	2.035
N1–C1	1.382(2)	N9–C33	1.372(2)	1.353
C1–C2	1.481(2)	C33–C34	1.464(2)	1.481
C2–C3	1.379(2)	C34–C35	1.392(2)	1.379
C3–C4	1.395(2)	C35–C36	1.396(2)	1.388
C4–C5	1.389(3)	C36–C37	1.409(3)	1.392
C5–C6	1.396(3)	C37–C38	1.389(3)	1.388
C6–C7	1.392(2)	C38–C39	1.400(2)	1.379
C2–C7	1.418(2)	C34–C39	1.404(2)	1.386
C7–C8	1.457(2)	C39–C40	1.463(2)	1.481
N1–C8	1.371(2)	N9–C40	1.372(2)	1.357
C8–N2	1.339(2)	C40–N10	1.342(2)	1.295
N2–C9	1.341(2)	N10–C41	1.340(2)	1.353
C9–C10	1.469(2)	C41–C42	1.464(2)	1.465
C10–C11	1.389(2)	C42–C43	1.403(2)	1.388
C11–C12	1.387(3)	C43–C44	1.395(2)	1.381
C12–C13	1.400(3)	C44–C45	1.409(3)	1.400
C13–C14	1.388(2)	C45–C46	1.395(3)	1.381
C14–C15	1.397(2)	C46–C47	1.392(2)	1.388
C10–C15	1.404(2)	C42–C47	1.402(2)	1.391
C15–C16	1.470(2)	C47–C48	1.476(2)	1.466
N3–C9	1.372(2)	N11–C41	1.364(2)	1.310
N3–C16	1.361(2)	N11–C48	1.379(2)	1.394
C16–N4	1.335(2)	C48–N12	1.316(2)	1.281
N4–C17	1.345(2)	N12–C49	1.343(2)	1.351
C17–C18	1.462(2)	C49–C50	1.447(2)	1.427
C18–C19	1.393(2)	C50–C51	1.397(2)	1.408
C19–C20	1.389(2)	C51–C52	1.381(3)	1.365
C20–C21	1.409(3)	C52–C53	1.403(3)	1.420
C21–C22	1.394(2)	C53–C54	1.386(3)	1.365
C22–C23	1.395(2)	C54–C55	1.406(2)	1.407
C18–C23	1.413(2)	C50–C55	1.406(2)	1.406
C23–C24	1.469(2)	C55–C56	1.469(2)	1.427
N5–C17	1.376(2)	N13–C49	1.372(2)	1.350
N5–C24	1.376(2)	N13–C56	1.369(2)	1.342
N6–C24	1.353(2)	N14–C56	1.357(2)	1.359
N6–C25	1.351(2)	N14–C57	1.349(2)	1.277
C25–C26	1.473(2)	C57–C58	1.484(2)	1.470
C26–C27	1.409(2)	C58–C59	1.397(2)	1.385
C27–C28	1.391(3)	C59–C60	1.387(3)	1.383
C28–C29	1.402(2)	C60–C61	1.395(3)	1.398
C29–C30	1.381(2)	C61–C62	1.387(3)	1.383
C30–C31	1.395(2)	C62–C63	1.389(2)	1.385
C26–C31	1.413(2)	C58–C63	1.401(2)	1.390
C31–C32	1.464(2)	C63–C64	1.467(2)	1.468
N7–C32	1.373(2)	N15–C64	1.377(2)	1.311
N7–C25	1.362(2)	N15–C57	1.372(2)	1.393
N8–C32	1.341(2)	N16–C64	1.332(2)	1.348
N8–C1	1.317(2)	N16–C33	1.334(2)	1.298

Table 3
Comparison of the coordination of the central Mg atom in 4+1 coordinated magnesium phthalocyaninato and porphyrinato complexes and in chlorophyll derivatives

Complex	Displacement of the Mg atom from the N_4-isoindole plane (Å)	Average Mg–N bond length (Å)	Mg–O bond length (Å)	Ref.
$MgPc(H_2O)$	0.442(3)	2.044	2.008(2)	This
(triclinic form) [a]	0.465(3)	2.046	2.036(2)	work
$MgPc(H_2O)$ (monoclinic form) [b]	~0.47	2.045	2.056(3)	[33]
$(MgPcH_2O)_2 \times 3py$	~0.45	2.037	2.013	[41]
$MgPc(H_2O) \times 2py$	0.496(4)	2.040	2.022	[40]
MgPc [c]	0.557(2)	2.047	–	[18]
$MgTPP(H_2O)$	0.273	2.072	2.099	[42]
$MgTPP(H_2O) \times 2(CH_3)_2CO$	0.45	2.083	2.054	[43]
$MgT(OMe)PP(H_2O)$	0.39	2.084	2.078	[44]
Ethyl chlorophyllide	0.39	2.086	2.035	[45]
Methyl chlorophyllide	0.34	2.78	2.030	[46]

[a] At 100 K.
[b] At 93 K.
[c] Data for MgPc at 120 K.

estimated energy of the intermolecular $Mg\cdots N_{azamethine}$ interaction in the dimers is ~40 kJ mol^{-1} and is nearly equivalent to the energy of the hydrogen bond [47]. This energy is significant and sufficient for the formation of the dimeric structure in the crystal of MgPc [18].

In the crystal the $MgPc(H_2O)$ molecules with the dipole moment of 5.36 D (the dipole moment was calculated for an isolated $MgPc(H_2O)$ molecule using the ab initio method [38] and the X-ray geometry of molecule) aligned along the Mg–O bonds form two centrosymmetric, but crystallographically different dimers via the intermolecular $O–H\cdots N_{azamethine}$ hydrogen bonds (Fig. 3) that stabilise the dimeric structure. Additionally the dimeric structure is also stabilised by the anti-parallel orientation of the dipole moments of $MgPc(H_2O)$ molecules. In the first dimer $(Mg1)_2$ the

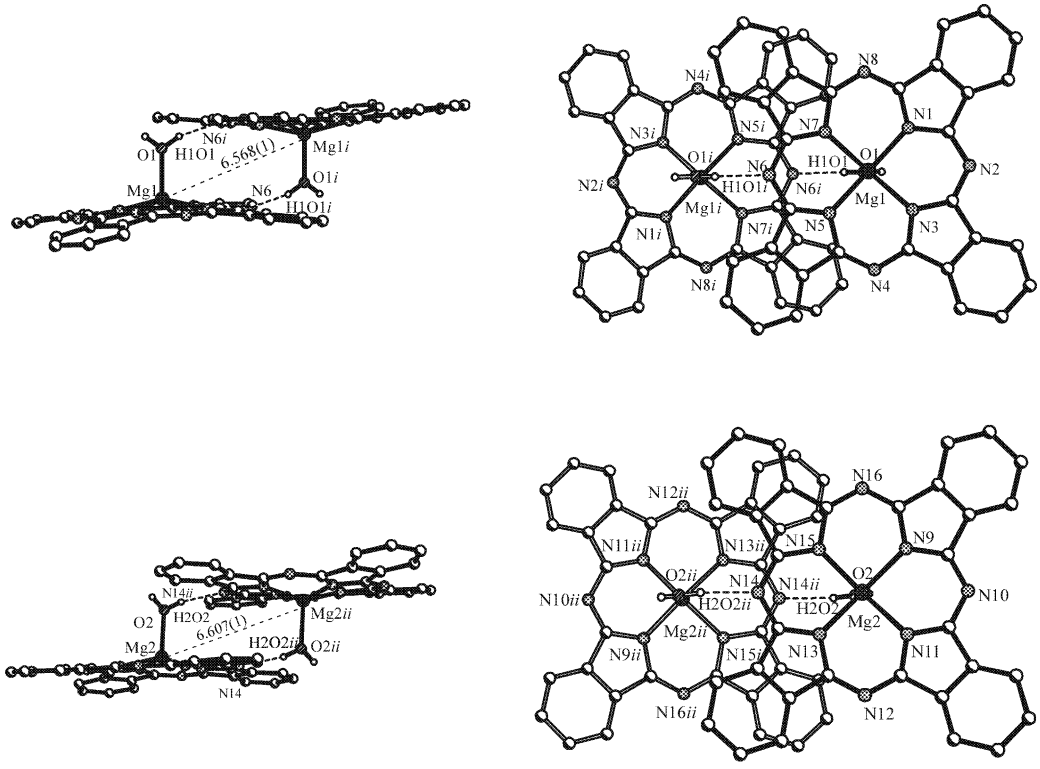

Fig. 3. View of the two crystallographically different dimeric structures of $[Mg1Pc(H_2O)]_2$ (top) and $[Mg2Pc(H_2O)]_2$ (bottom), side view (left) and top view (right).

Table 4
Hydrogen bonding geometry (Å, °) in the $MgPc(H_2O)$ dimeric structure

D–H···A	d(D–H)	d(H···A)	d(D···A)	<(D–H···A)
O1–H1O1···N6^{i}	0.85(2)	2.01(2)	2.831(2)	164(2)
O2–H2O2···N14^{ii}	0.83(2)	1.95(2)	2.763(2)	165(2)
O1–H2O1···N10	0.83(2)	2.15(2)	2.975(2)	171(2)
O2–H1O2···N6^{i}	0.77(2)	2.49(2)	3.232(2)	162(2)

The first two lines relate the hydrogen bonds in dimers, the second two lines relate the hydrogen bonds between the dimers. *Symmetry code:* i, $-x+1$, $-y$, $-z+1$; ii, $-x+1$, $-y$, $-z$.

distance of D···A (donor···acceptor) is equal to 2.831(2) Å and in the second dimer $(Mg2)_2$ it is equal to 2.736(2) Å (see Table 4). Thus the $MgPc(H_2O)$ molecules in the dimer $(Mg2)_2$ interact stronger than in dimer $(Mg1)_2$. The interactions in the dimers correlate well with the distances between the N_4-isoindole planes of the dimers. These distances are equal to 3.367(3) and 3.224(3) Å in the dimer of $(Mg1)_2$ and $(Mg2)_2$, respectively. As mentioned similar dimers (Fig. 4) also exist in the crystals of MgPc [18]. A comparison of the geometry of the $(MgPc)_2$ and $[MgPc(H_2O)]_2$ dimers is collected in Table 5. The interplanar distances in the dimers are shorter than the van der Waals distance of $\sim$3.4 Å for the aromatic carbon atoms [48] and indicate strong π–π interactions between the partially overlapped phthalocyaninato(2-) rings. This interaction leads to appreciable distortion of the phthalocyaninato(2-) rings from planarity. The extent of the molecular distortions can be described by the angles between the plane of four central *N*-isoindole atoms and the plane of each isoindole moiety and by the angles between the planes of pyrrole and benzene rings. These angles are listed in Table 6.

The crystals of aquamagnesium phthalocyanine are built up from two crystallographically different $[MgPc(H_2O)]_2$ dimers (see Fig. 3). The arrangement of the dimers of $[MgPc(H_2O)]_2$ in the crystal is illustrated in Fig. 5a. The dimers are stacked in a herringbone fashion along the *b*-axis. Two kinds of stacking column are present in the crystal: one column is composed of only $(Mg1)_2$ dimers, the other of only $(Mg2)_2$ dimers. Besides the strong π–π interaction between the phthalocyaninato rings in the dimers, the π–π interaction between dimers along the columns is also important. The interplanar spacing between the back-to-back phthalocyaninato(2-) rings of the dimers is comparable to the distance of 3.4 Å for the interacting aromatic ring system [48]. The dihedral angle between the phthalocyaninato(2-) planes of the $(Mg1)_2$ and $(Mg2)_2$ dimers is equal to $\sim$65.5°. The pattern of the arrangement of the $[MgPc(H_2O)]_2$ dimers resembles the arrangement of the $(MgPc)_2$ dimers in the crystal of β modification of MgPc [18] (see Fig. 5b).

Table 5
Comparison of the $(MgPc)_2$ and $[MgPc(H_2O)]_2$ dimers present in the crystals

Dimer	$[MgPc(H_2O)]_2$ [a]	$(MgPc)_2$ [b]
Deviation of the Mg atom from the N_4-isoindole plane, (Å)	0.442(3)	0.557(2)
	0.465(3)	0.461(2)
		0.431(2)
Distance between the N_4-isoindole planes, (Å)	3.367(3)	3.172(2)
	3.2239(3)	3.183(2)
		3.185(2)

[a] The first line relates to $(Mg1)_2$, second line to $(Mg2)_2$ dimer.
[b] The values reported in the first, second and third lines relate the structure at 120, 200 and 260 K, respectively.

3.3. Gas-phase structure of $MgPc(H_2O)$

The ab initio full-optimised molecular orbital calculations [38] gave bond distances and angles, which are in general in good agreement with those obtained from the X-ray structure investigation (Table 2). A noticeable

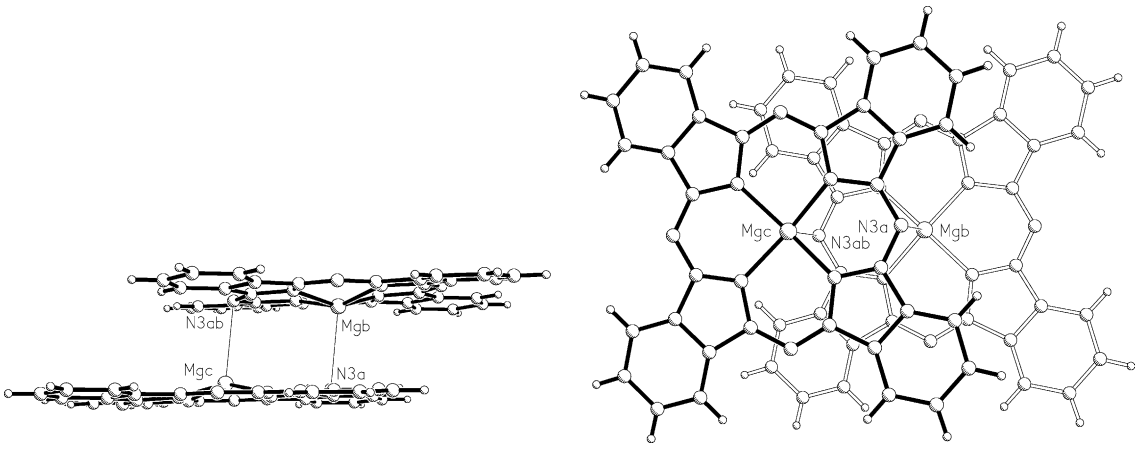

Fig. 4. Side and top view of the dimers of $(MgPc)_2$.

Table 6
Molecular distortion of the phthalocyaninato(2-) ring in the triclinic and monoclinic crystals of $MgPc(H_2O)$ and in the crystal of β-MgPc

The angle between the N_4-isoindole plane and the isoindole moieties, (°)						
Plane 1 (N_4-plane)	Plane 2 (isoindole plane)	Triclinic form		Optimised geometry	Monoclinic form [33]	β-MgPc
		Molecule 1	Molecule 2			
N1, N3, N5, N7	N1, C1–C8	12.3		5.4	2.1	2.8
N9, N11, N13, N15	N9, C33–C40		3.9			
N1, N3, N5, N7	N3, C9–C16	5.6		7.2	1.8	4.2
N9, N11, N13, N15	N11, C41–C48		12.0			
N1, N3, N5, N7	N5, C17–C24	1.5		5.0	0.3	−2.8
N9, N11, N13, N15	N13, C49–C56		7.9			
N1, N3, N5, N7	N7, C25–C32	6.4		5.2	1.8	−4.2
N9, N11, N13, N15	N15, C57–C64		1.4			
The angle between the planes of pyrrole and benzene rings, (°)						
(pyrrole plane)	(benzene plane)					
N1, C1, C2, C7, C8	C2–C7	2.1		0.0	2.1	2.0
N9, C33, C34, C39, C40	C34–C39		0.5			
N3, C9, C10, C15, C16	C10–C15	0.5		0.8	0.9	1.6
N11, C49, C50, C55, C56	C50–C55		3.1			
N5, C17, C18, C23, C24	C18–C23	1.9		0.2	1.6	−2.0
N13, C41, C42, C47, C48	C42–C47		2.3			
N7, C25, C26, C31, C32	C26–C31	1.6		0.2	2.9	−1.6
N15, C57, C58, C63, C64	C58–C63		2.3			

For the labelling of the atoms—see Fig. 2.

difference can be found in the slightly shorter displacement of the central magnesium atom from the N_4-isoindiole plane: 0.401 Å in the optimised molecule and 0.442(3) and 0.465(3) Å for Mg1 and Mg2, respectively, in the crystal. The optimised Mg–N distances and the N–Mg–N and N–Mg–O angles (see Table 7) are comparable with those in the crystal. However, the greatest difference between the gas-phase and X-ray geometry of $MgPc(H_2O)$ molecule is observed in the Mg–O bond distance (see Table 2). The optimised Mg–O bond distance is greater than the Mg–O bond in both crystallographically independent $MgPc(H_2O)$ molecules. The calculated energy of the Mg–O bond is equal to ∼ 130 kJ mol^{-1}. This correlates well with the thermogravimetric experiment that shows a moderately stable Mg–O bond during temperature treatment. This value is greater than the energy of the Mg–O bond in $MgPc(H_2O)(NMP)_2$ (NMP = *N*-methyl-2-pyrrolidone) and MgPc(2-methoxyethanol)$_2$, both well characterised 4+2 coordinated magnesium phthalocyaninato complexes [32] in which the calculated Mg–O bond energies are equal to 60–78 and 69–87 kJ mol^{-1}, respectively

Table 7
Gas-phase optimised and X-ray Mg coordination parameters (Å, °) of $MgPc(H_2O)$

	Triclinic modification		Monoclinic modification [33]	Optimised geometry
	Molecule 1	Molecule 2		
Mg1(2)–O1(2) [a]	2.0076(14)	2.0357(14)	2.056(3)	2.142
Mg1(2)–N1(9)	2.0380(15)	2.0468(15)	2.046(4)	2.039
Mg1(2)–N3(11)	2.0419(14)	2.0455(15)	2.048(4)	2.037
Mg1(2)–N5(13)	2.0477(15	2.0396(15)	2.038(4)	2.025
Mg1(2)–N7(15)	2.0488(15)	2.0470(15)	2.025(4)	2.035
Deviation of Mg from N_4-plane	0.442(3)	0.456(3)	0.47	0.401
O1(2)–Mg1(2)–N1(9)	102.28(6)	105.43(6)	106.8(1)	106.2
O1(2)–Mg1(2)–N3(11)	104.08(6)	104.88(6)	101.1(2)	100.3
O1(2)–Mg1(2)–N5(13)	103.07(6)	101.26(6)	99.8(2)	96.4
O1(2)–Mg1(2)–N7(15)	100.53(6)	100.97(6)	105.6(2)	102.8
N1(9)–Mg1(2)–N3(11)	86.90(6)	86.26(6)	87.9(2)	86.5
N3(11)–Mg1(2)–N5(13)	87.81(6)	88.50(6)	88.4(2)	89.1
N5(13)–Mg1(2)–N7(15)	85.90(6)	85.48(6)	85.6(1)	88.6
N1(9)–Mg1(2)–N7(15)	88.66(6)	87.89(6)	85.9(2)	86.5

[a] The number in parentheses relates the numbering for molecule 2 (triclinic form).

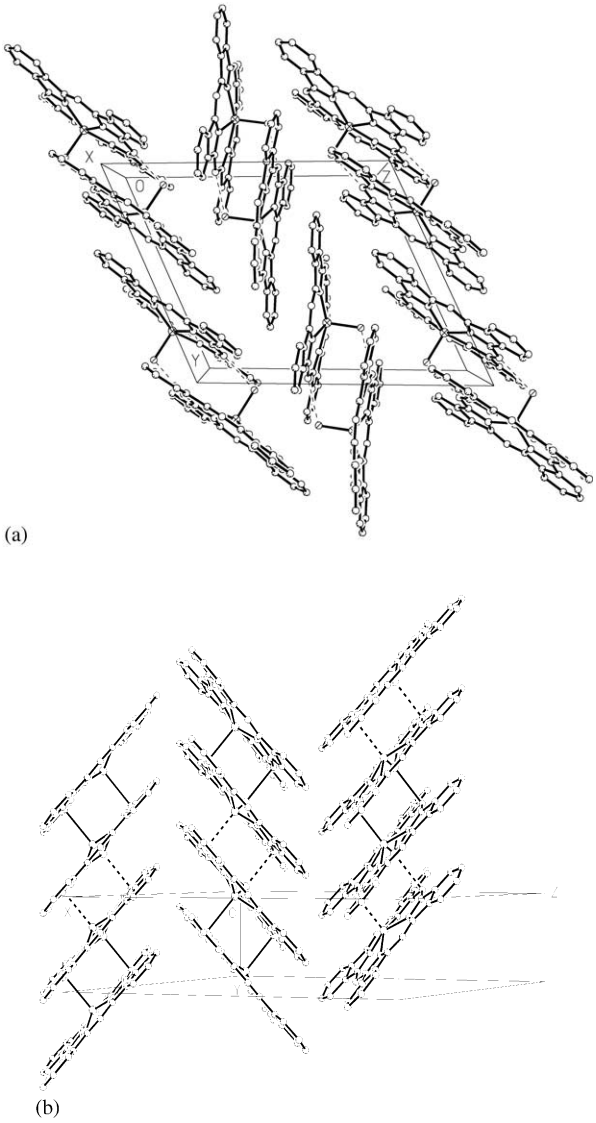

Fig. 5. Molecular arrangement of the $[MgPc(H_2O)]_2$ (a) and the $[MgPc]_2$ (b) dimers in the unit cell. Due to the symmetry of the crystal of β-MgPc the dimer $[MgPc]_2$ as the basic subunit is statistically disordered in the crystal (solid line —50%, dashed line—50% in figure (b)).

[48]. The difference in the energies of the Mg–O bonds correlate well with the Mg–O bond lengths in the crystals: in $MgPc(H_2O)$ the Mg–O bond length is much shorter (2.022 Å) than in both complexes $MgPc(H_2O)(NMP)_2$ (2.171(5) Å) and $MgPc(2\text{-methoxyethanol})_2$ (2.244(6) Å) [32]. The energy of the Mg–O bond in the crystal of $MgPc(H_2O)$ is approximately one-half the energy of the Mg–N bond ($\sim$290 kJ mol^{-1}) [48]. The shorter Mg–O bond in the crystal than in the optimised molecule is undoubtedly due to the formation of the hydrogen-bonded dimeric structure as well as the strong π–π interaction between the phthalocyaninato(2-) rings. A similar relation between the X-ray and optimised Mg–O bond length has been reported for the aquamagnesium tetra(methoxyphenyl)porphyrin molecule [44], in which the optimised Mg–O bond length of 2.141 Å is longer than the one in the crystal (2.078(12) Å). Looking at the X-ray experimental and optimised geometrical parameters of the $MgPc(H_2O)$ molecule in more detail (see Tables 2, 6 and 7) it can be stated that the distortion of the phthalocyaninato(2-) ring of the $MgPc(H_2O)$ molecule is greater in the crystal than in the optimised structure (Table 6). The distortion of the phthalocyaninato(2-) ring in the gas-phase is not symmetric, the dihedral angles between the N_4-plane and the plane of each isoindole moiety are not equal (ranging from 5.0° to 7.2°). These differences are likely due to the interaction of the π-cloud of the phthalocyaninato(2-) ring with the hydrogen atoms of the coordinated water molecule, and due to the interaction of the π-cloud of the Pc(2-) ring with the lone pair of electrons of the oxygen atom. The former interaction leads to the greater value of the dihedral angle between the N_4-plane and the N3,C9–C16 isoindole moiety (7.2°), since the lone pair of electrons on the oxygen atom is oriented in this direction. The asymmetric distortion of the Pc(2-) ring of the $MgPc(H_2O)$ molecule in the gas-phase is in agreement with the valence-shell electron pair repulsion model (VSEPR) that predicts more space for the lone pair of electrons than for the bonding electron pair [49,50]. The distortion of the phthalocyaninato(2-) ring in the crystal of the second modification (monoclinic) of $MgPc(H_2O)$ (see Table 6) is significantly smaller than in the optimised $MgPc(H_2O)$ molecule. This is in contrast to our expectation, since in general the molecular distortion in the crystal is greater than in the optimised molecule, due to the intermolecular interactions in the crystal as well as the crystal packing forces. This can be explained by the difference in the crystal packing and the arrangement of $MgPc(H_2O)$ molecules in the crystal, that in contrast to the triclinic modification, do not form the dimers, but the molecules in the crystal form a more loose hydrogen-bonded polymeric structure [33]. On the other hand, the final refinement parameters of 10.6 and 20.9% for R and $wR(F^2)$ for the monoclinic modification are relatively high due to the poor quality of the single crystal [33], so the precision of the geometrical parameters is rather low.

3.4. Vibrational spectroscopy

Fig. 6 shows the IR spectrum of $MgPc(H_2O)$ in KBr pellet, and Table 8 lists the positions of the most prominent bands. The table contains also the spectral data for the MgPc complex [51–53]. The main IR bands correspond to the characteristic vibrations of the phthalocyaninato macrocycle, which are well described in the literature for the metal-free phthalocyanine [51,54,55]. In the spectral region of 1600–1250 cm^{-1} the C–C and C–N stretching modes from benzene and pyrrole rings dominate, yielding peaks with contribu-

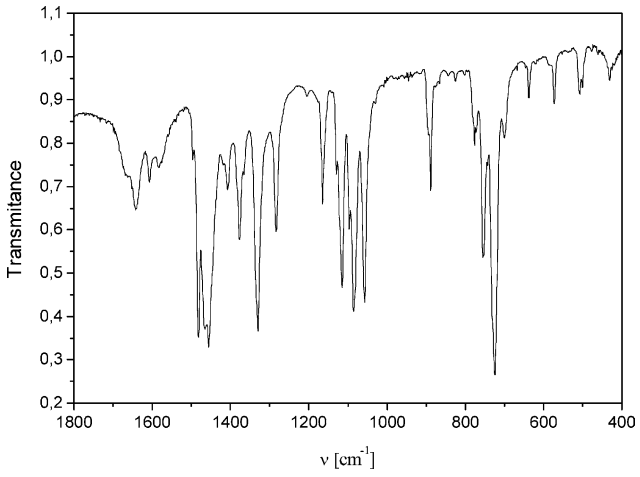

Fig. 6. Infrared spectrum of the $MgPc(H_2O)$ complex.

Table 8
IR spectral data for $MgPc(H_2O)$

$MgPc(H_2O)$	MgPc	Assignment
432w	431	ϕ(C–C) macrocycle ring deformation
500w	502	ϕ(C–C) macrocycle ring deformation
508w		
573w	571	ϕ(C–C) macrocycle ring deformation
638w	638	ϕ(C–C) macrocycle ring deformation
699m	–	$\gamma(H_2O)$ of coordinated water molecule
725vs	722	γ(C–H) out-of-plane deformation
755s	754	γ(C–H) out-of-plane deformation
777m	771	γ(C–N) stretching
889m	890	γ(C–H) out-of-plane deformation
1030w	1027	β(C–H) in plane deformation
1058w	1058	β(C–H) in plane deformation
1086s	1082	ν(C–N) stretching in pyrrole
1097m		
1116s	1113	β(C–H) in plane deformation
1166m	1163	ν(C–N) in plane
1283m	1282	ν(C–N) in isoindole
1330s	1327	ν(C–C) in isoindole
1370m	1361	ν(C–C) in isoindole
1408w	1407	ν(C–C) in isoindole
1456s	1451	ν(C–C) in isoindole
1466s		
1482s	1479	ν(C–C) in isoindole
1583w	1584	ν(C–C) in pyrrole
1607w	1608	ν(C–C) in isoindole
1642m		$\delta(H_2O)$ of coordinated water molecule
1667w		
3080w,sh		O–H···N in dimers
3358m		ν_s of coordinated water molecule
3419m		ν_a of coordinated water molecule

v, Very; s, strong; m, medium; w, weak; sh, shoulder.

tions from both $\nu_{(C-C)}$ and $\nu_{(C-N)}$ modes. The region of 1250–1000 cm^{-1} is characteristic for the C–H in-plane bending mode ($\beta_{(C-H)}$) of the aromatic phthalocyaninato ring. In the 1000–800 cm^{-1} spectral region the bands are attributed to the $\gamma_{(C-H)}$ out-of-plane vibrational modes, and below 800 cm^{-1} mainly the $\phi_{(C-C)}$ deformation modes of macrocycle are observed. The differences in the IR frequencies of the phthalocyaninato macrocycle between $MgPc(H_2O)$ and MgPc are very small. These correlate well with the strengths of the bonds and are consistent with the C–C, C–N, C–H and Mg–N bond lengths in both structures (the central Mg atom in both crystals is displaced from the Pc-macrocyle), thus the equivalent IR bands remain unaffected.

As can be seen from Table 8, the IR spectrum of $MgPc(H_2O)$ in relation to the spectrum of MgPc differs only in the regions where the expected vibrational modes of coordinated water molecule are present. Thus the bands at 3358 and 3419 cm^{-1} correspond to symmetric and asymmetric (ν_s, ν_a) vibrations of coordinated water molecule. Similarly two vibrational peaks at around 3400 cm^{-1} were observed in the spectrum of chlorophyll treated with water [56–58]. The δ vibrational mode of coordinated water molecule is observed as a medium band at 1642 cm^{-1}. Additionally the band at 699 cm^{-1} is attributed to the $\gamma(H_2O)$ mode of the coordinated water molecule. All IR bands related to the coordinated water molecule were not observed in the spectrum of MgPc [51–53]. The observed splitting of some peaks in the spectrum of $MgPc(H_2O)$ in relation to the spectrum of MgPc are in agreement with the change in symmetry of the $MgPc(H_2O)$ molecule in relation to the symmetry of MgPc (due to the displacement of the central Mg atom from the Pc-plane in the MgPc, the symmetry of MgPc is C_{4v} and the symmetry of $MgPc(H_2O)$ is approximately C_{2v}). Stymne et al. [59] and Sidorov and Kotlyar [60] investigated the change of the IR spectrum of MgPc upon exposure to water, but the changes in the IR spectrum are attributed improperly, since they suggested that the water molecule is joined by O–H···N hydrogen bonds with the azamethine nitrogen atom of the phthalocyaninato macrocycle and is not coordinated to the central Mg atom. This is in contrast to our X-ray investigation that clearly shows that the water molecule is directly joined to the central Mg atom of MgPc yielding the 4+1 coordinated $MgPc(H_2O)$ complex. Additionally, a multicomponent broad band located at approximately 3080 cm^{-1} arising from a set of weak interactions of hydrogen O–H···N bonds is observed. This is in agreement with the X-ray single crystal analysis, which shows that the $MgPc(H_2O)$ molecules form hydrogen-bonded dimeric structures.

The far infrared spectra of metal-free phthalocyanine and several metallophthalocyanines have been studied [61–64], especially the assignment of the metal dependant bands. Kobayashi [63] analysed the far infrared spectra of several metal(II) phthalocyaninato complexes (M(II) = Fe, Co, Ni, Cu, Zn, Pd, Pt) by a comparison with the spectrum of metal-free phthalocyanine and assigned the metal-ligand vibrational mode. Clarisse and Riou [64] in similar way have assigned the bands to metal-ligand vibrations in some diphthalocyaninato complexes. The far infrared spectrum of $MgPc(H_2O)$ is

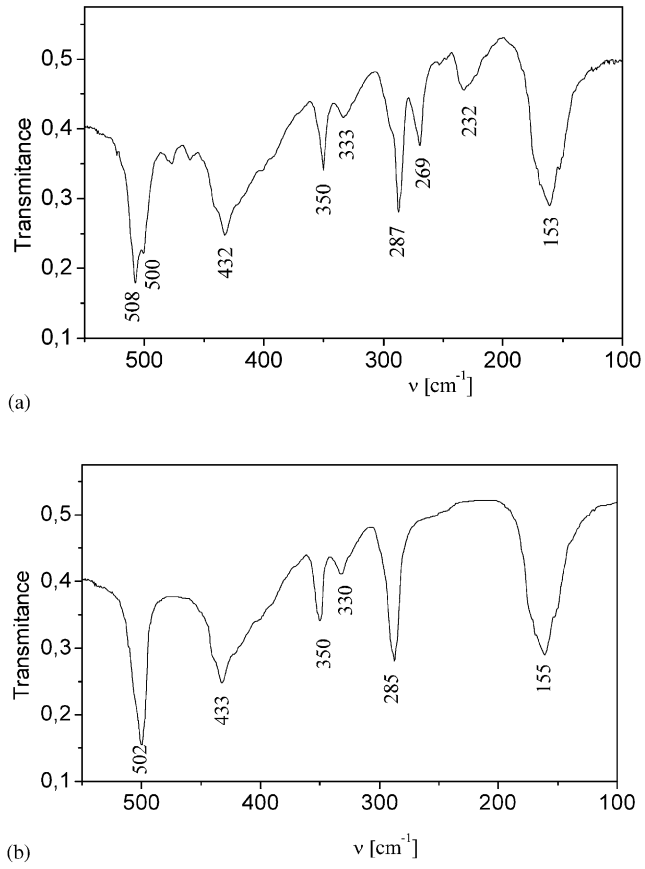

Fig. 7. Far infrared spectrum of the $MgPc(H_2O)$ complex (a) and β-MgPc (b).

illustrated in Fig. 7(a) with the frequencies of the most prominent bands. The bands at approximately 500 and at 432 cm^{-1} are originated from the ϕ(C–C) macrocycle ring deformations. According to Terzian et al. [65] the band at 350 cm^{-1} is assigned to metal dependent isoindole ring deformation and the bands at 287 and 153 cm^{-1} are assigned to ν(Mg–N) and ν(N–Mg–N) vibrational modes, respectively. The band at 269 cm^{-1} that is not observed in the spectrum of MgPc (Fig. 7(b)) we assigned to the Mg–O vibration, since as shown by the X-ray structure analysis the Mg–N bond distance is comparable to the distance of the Mg–O bond. Comparing the far infrared spectra of $MgPc(H_2O)$ and MgPc it should be stated that the frequencies of equivalent bands attributed to the same vibrational modes are very similar, thus the coordination of a water molecule by MgPc does not affect the strength of the bonds of the aromatic phthalocyaninato(2-) macrocycle. The weak band at 232 cm^{-1} which is observed only in the spectrum of $MgPc(H_2O)$ is undoubtedly originated from the stretching vibration of the O–H···N bridge of the dimers of $[MgPc(H_2O)]_2$, since the band assigned to the O–H···N and O–H···O bridges was observed at about 230 cm^{-1} in the spectra of other compounds [66]. This assignment is fully consistent with the X-ray structure analysis.

3.5. UV–vis spectroscopy

Since the $MgPc(H_2O)$ complex is stable only up to about 200 °C as shown by the thermogravimetric experiment (see Fig. 1), the preparation of a solid state thin film using a standard technique, i.e., thermal evaporation, was impossible due to the loss of water from $MgPc(H_2O)$ molecules. Therefore, the solid state thin film was prepared from a nujol mull of $MgPc(H_2O)$. The solid state UV–vis spectrum of $MgPc(H_2O)$ is illustrated in Fig. 8(a), which also shows the spectrum in pyridine solution. The solid state spectrum of the triclinic modification of $MgPc(H_2O)$, contrary to that of the monoclinic form [33] and to our expectations, is very similar to the UV–vis spectrum of the literature X-phase of the magnesium phthalocyaninato complex (the near-IR active phase) that has been reported many times (for example see Figure 1 in Ref. [31]). Thus the intense absorption band (Fig. 8(a)) is typical for the solid state, since the spectrum of $MgPc(H_2O)$ in pyridine solution shows as expected only one single peak—the Q band which originates from the excitation between the HOMO (a_2, π) ground state (according to the C_{4v} symmetry of the $MgPc(H_2O)$ molecule in solution) and

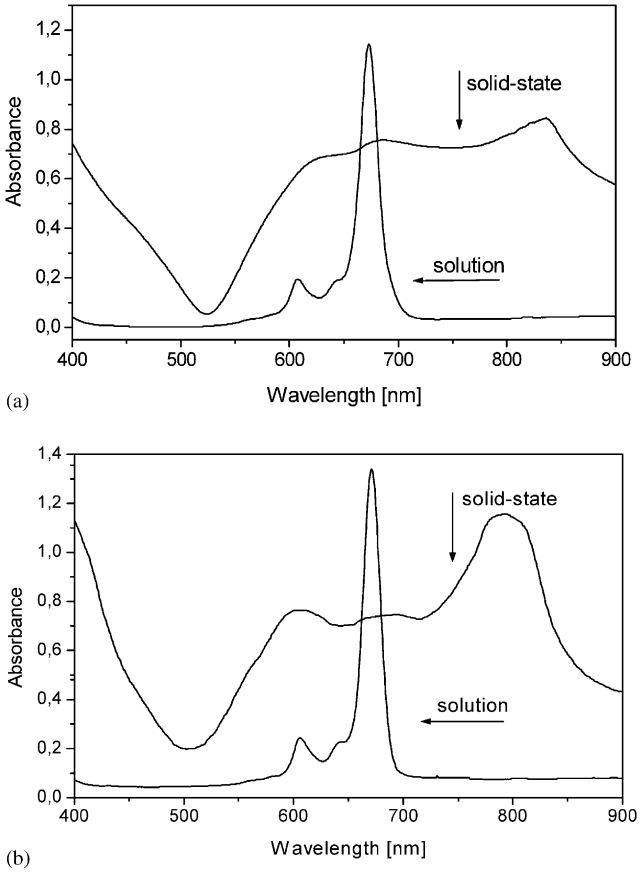

Fig. 8. UV–vis spectra of the triclinic form of $MgPc(H_2O)$ in solid state and in pyridine solution (a) and β-MgPc in solid state and in pyridine solution (b).

the LUMO (e, π*), the first doubly degenerate excited state. Additionally, as can be seen from Fig. 8(a), the Q band exhibits characteristic splitting due to the vibronic coupling in the excited state, which is well known and described in the literature [67,68].

The solid state thin film of the β-MgPc complex was prepared in the same manner (from a nujol mull) and its UV–vis spectrum is illustrated in Fig. 8(b) together with the spectrum in pyridine solution. Thus the effects of the different treatments of the samples during preparation of the thin solid films or the different solvents (for the spectra in solution) were eliminated. The optical solid state properties of $MgPc(H_2O)$ and β-MgPc complexes, contrary to our expectation, are very similar, both showing the intense absorption band in the spectral region of 500–900 nm that is characteristic for the spectrum of the X-phase of the magnesium phthalocyaninato complex. Our UV–vis experiments clearly show that the intense absorption band in the spectrum of $MgPc(H_2O)$ as well as of β-MgPc originates from the molecular arrangement and the intermolecular interactions present in the solid state (in the crystals), since the UV–vis spectra of both complexes in pyridine solution are identical. Thus in pyridine solutions both complexes, $MgPc(H_2O)$ and MgPc, should exist in the same form.

Our investigations of $MgPc(py)_2$ show that this complex, in which the two pyridine molecules are axially coordinated to the central Mg atom of the MgPc molecule, in pyridine solution transforms into $[MgPc(H_2O)] \times 2py$, and after several days single crystals of this complex appear from the solution [39]. Crystals of $[MgPc(H_2O)] \times 2py$ can also be obtained from MgPc in pyridine solution under ambient atmosphere, since the pyridine under these conditions (under moist atmosphere) always contains water as an impurity. Thus in the pyridine solution of both Mg complexes, i.e., $MgPc(H_2O)$ and MgPc, the complex of $[MgPc(H_2O)] \times 2py$, exists as the most stable form (see Scheme 1), therefore the UV–vis spectra in pyridine solution are identical (see Fig. 8(a) and (b)).

The intense absorption band observed in the spectrum of solid state triclinic modification $MgPc(H_2O)$ as well as in the spectrum of β-MgPc originates from the molecular arrangement and intermolecular interactions present in the crystals that lead to the distortion of the Pc macroring. The distortion of the Pc ring is well known to lift the degeneracy of the excited state to influence the optical properties [69]. Therefore the extent of the molecular distortion was discussed in detail in the description of the structure and is summarised in Table 6 together with the distortions of the Pc ring of $MgPc(H_2O)$ in the monoclinic crystal and in the crystal of β-MgPc. The optimised geometry, which corresponds to the conformation of the molecule in solution, of the $MgPc(H_2O)$ molecule has approximately C_{4v} symmetry. Thus the excited state is doubly degenerate and the $\pi \rightarrow \pi^*$ transition ($a_2 \rightarrow e$) yields an expected single strong peak as observed in solution. Upon crystallisation the degeneracy of the excited state is lifted due to the molecular distortion (C_1 symmetry of $MgPc(H_2O)$ molecule in the crystal) and induces a band splitting. However, as shown in the theoretical calculations performed for two 4+2 coordinated magnesium phthalocyaninato complexes [31] and for MgPc [70] the splitting value is relatively small ($\sim$10 nm) in relation to the observed broad band and is proportional to the distortion of the phthalocyaninato macrocycle. As can be seen from Table 6, the distortion of the Pc ring of both independent $MgPc(H_2O)$ molecules in the crystal (triclinic) is very similar to, but greater than the distortion of the Pc ring of the $MgPc(H_2O)$ molecule in the monoclinic crystal. The distortions of the Pc ring of $MgPc(H_2O)$ molecules in the triclinic crystal are comparable to those reported for the crystal of $[MgPc(H_2O)_2](NMP)_2$ in which the calculated splitting value due to molecular distortion is only 11.1 nm [31], so the molecular distortion is not the main reason responsible for the observed very broad intense absorption band in the spectral region of 500–900 nm. Additionally, the molecular distortion does not explain the existence of the broad absorption band in the spectrum of β-MgPc (see Fig. 8(b)) because the distortion of the Pc ring in the crystal is significantly smaller than that observed for the triclinic form of $MgPc(H_2O)$ and comparable to that observed in the monoclinic form of $MgPc(H_2O)$ (see Table 6) whose solid state spectrum does not show the intense broad absorption band reported by Mizuguchi [33]. For this reason we suggest that a much more important role in the origin of the intense broad absorption band is played by the π–π interactions and the arrangement of $MgPc(H_2O)$ molecules in the crystal that form dimers via the O–H···N hydrogen bonds between the anti-parallel oriented dipole $MgPc(H_2O)$ molecules (see Figs. 3 and 5). Both solid state spectra of $MgPc(H_2O)$ and β-MgPc complexes show a similar broad intense band due to the strong π–π interactions and similar arrangement of molecules in the crystal. The MgPc molecule as shown by the X-ray single crystal analysis [18] is non-planar, the Mg atom being displaced from the Pc plane by $\sim$0.5 Å due to the interaction with the *N*-azamethine atom of a neighbouring MgPc molecule. This interaction leads to the formation of $(MgPc)_2$ dimers, which are arranged in the crystal in a similar manner as the dimers of $MgPc(H_2O)$ molecules (in the triclinic crystal). The arrangement of dimers ($[MgPc(H_2O)]_2$ and $(MgPc)_2$) in the solid state (crystals) and the π–π interactions are responsible for the broad intense absorption band.

The suggestion that the formation of the dimers in the crystal with strong π–π interactions between the Pc rings is responsible for the observed intense absorption is in agreement with the arrangement of $MgPc(H_2O)$

molecules in the monoclinic crystal that do not form dimers (see Fig. 9), in that the solid state spectrum of the monoclinic modification of $MgPc(H_2O)$ does not show the intense broad absorption band [33]. Additionally, it should be added that a similar intense absorption band is observed in the solid state spectra of titanyl phthalocyanine, OTiPc, (phase II and Y) [69,71–73] and vanadyl phthalocyanine, OVPc, (Phase II) [74–76]. Vanadyl phthalocyanine (OVPc) crystallises in two different modifications: monoclinic—phase I and triclinic—phase II, but the crystal structure on a single crystal is known only for phase II [77]. Phase I (monoclinic) has been identified by the powder diffraction method [78]. The crystal structures of titanyl phthalocyanine (phase I and II) have been determined on single crystals [79], while the third phase of OTiPc (phase Y) was determined by Rietveld analysis on the basis of powder diffraction [80]. The crystal structures of phase II (triclinic) of titanyl and vanadyl phthalocyanines clearly show that the OTiPc and OVPc molecules in the crystals are arranged in the face-to-face manner similar to $MgPc(H_2O)$ molecules in the triclinic crystal. The monoclinic phase I of OTiPc and OVPc, similarly to the monoclinic form of $MgPc(H_2O)$, have no active form in the near-IR region. In phase II (triclinic) the distortion of the Pc ring of both titanyl and vanadyl phthalocyanines (see Table 9) is very similar to the distortion of the Pc ring in the triclinic crystal of $MgPc(H_2O)$. The distortion of the Pc ring is undoubtedly due to the same face-to-face arrangement of molecules as the arrangement of $MgPc(H_2O)$ molecules that form dimers. Thus the $\pi-\pi$ interaction between the Pc rings of the 'dimeric' structure of OTiPc and OVPc (the Pc–Pc distance of ~ 3.2Å is comparable to that found in the dimers of triclinic modification $MgPc(H_2O)$. Therefore the intense broad absorption band observed in the solid state spectrum of these phthalocyaninato complexes originates from the anti-

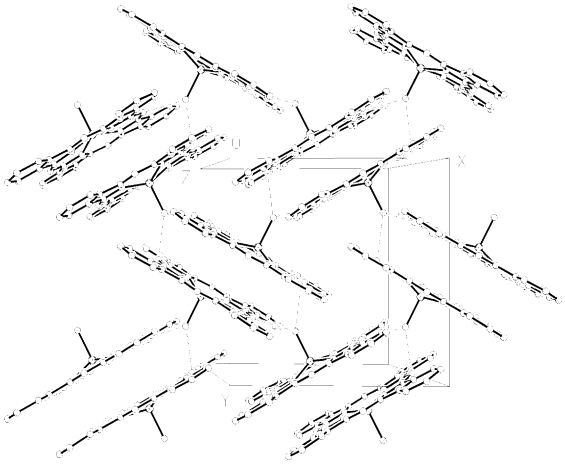

Fig. 9. Arrangement of $MgPc(H_2O)$ molecules in the monoclinic crystal (using coordinates of the atoms given in Ref. [33]).

Table 9
Comparison of the distortion of the phthalocyaninato(2-) ring in the crystals of some metallophthalocyaninato complexes

		Near-IR active				Near-IR inactive	
Plane 1	Plane 2	$MgPc(H_2O)$ triclinic [a]	OTiPc phase II triclinic	OTiPc phase Y triclinic	OVPc phase II triclinic	$MgPc(H_2O)$ monoclinic	OTiPc phase I monoclinic
N1, N3, N5, N7	C2–C7	13.2/13.3	11.8	11.8	11.2	2.4	7.7
N1, N3, N5, N7	C10–C15	5.6/3.5	6.2	6.2	6.1	1.8	6.5
N1, N3, N5, N7	C18–C23	2.0/2.1	1.2	1.2	10.8	0.4	5.8
N1, N3, N5, N7	C26–C31	6.7/8	7.9	7.8	7.1	3.0	6.1
Reference		this work	[78]	[80]	[77]	[33]	[78]

Plane 1, N_4-isoindole; Plane 2, each of phenyl ring of Pc.
[a] The values reported distortion for both independent $MgPc(H_2O)$ molecules in the crystal.

parallel arrangement of polar phthalocyaninato molecules (the dipole moment of these molecules is aligned along the M–O bond) that form the dimeric structure with the strong π–π interactions between the Pc rings, while the distortion of the Pc rings plays a lesser role. This suggestion also explains why the solid state spectrum of β-MgPc also shows a similar broad absorption band (dimeric structure of β-MgPc).

4. Conclusions

i) MgPc(H_2O) crystallises in the monoclinic or triclinic system depending on the crystallisation conditions.
ii) Only the triclinic modification has a near-IR active form.
iii) The intense broad absorption band is observed only on the solid state samples.
iv) The intense broad absorption band mainly originates from the molecular arrangement in the crystal with strong π–π interactions between the Pc rings in the dimers.
v) The intense broad absorption band in the solid state UV–vis spectrum of β-MgPc also originates from the dimeric structure of $(MgPc)_2$ with strong π–π interactions between the Pc rings.
vi) The suggestion in the literature that the near-IR active X-phase of magnesium phthalocyanine contains two water molecules is not confirmed, since the near-IR activity of magnesium phthalocyanine ($MgPcH_2O$ or MgPc) is closely related with the molecular arrangement—the dimeric structure with strong π–π interactions between the Pc rings.

5. Supplementary material

Additional material comprising full details of the X-ray data collection and final refinement parameters including anisotropic thermal parameters and a full list of the bond lengths and angles have been deposited with the Cambridge Crystallographic Data Center in the CIF format as supplementary publications CCDC No. 194384. Copies of the data can be obtained free of charge on application to The Director, CCDC, 12 Union Road, Cambridge, CB2 1EZ, UK (fax: +44-1223-336033; email: deposit@ccdc.cam.ac.uk or www: http://www.ccdc.cam.ac.uk).

Acknowledgements

The authors thanks the CNPq foundation for financial support and Prof. Dr E.E. Castellano from the Instituto de Física de São Carlos, Universidade de São Paulo for the opportunity to make the data collection on the Enraf-Nonius Kappa-CCD diffractometer in his laboratory.

References

[1] A.L. Thomas, Phthalocyanine Research and Application, CRC Press, Boca Raton, 1990.
[2] N.B. McKeown, Phthalocyanine Materials: Synthesis, Structure and Function, Cambridge University Press, Cambridge, 1998.
[3] R.O. Loutfy, A.M. Hor, G. DiPaola-Barnyi, C.K. Hsiao, J. Imag. Sci. 19 (1985) 116.
[4] W. Herbst, K. Hunger, Industrial Organic Pigments, New York, VCH, 1993.
[5] N.C. Khe, M. Aizawa, Nippon Kagaku Kaishi (1986) 393.
[6] T. Daidoh, H. Matsunaga, K. Iwata, Nippon Kagaku Kaishi (1988) 1090.
[7] A.K. Gosh, D.L. Morel, T. Feng, R.F. Shaw, C.A. Rowe, J. Appl. Phys. 45 (1974) 230.
[8] A.B.P. Lever, M.R. Hempstead, C.C. Leznoff, W. Lin, M. Melnik, W.A. Nevin, P. Seymour, Pure Appl. Chem. 58 (1986) 1467.
[9] E. Orti, J.L. Bredas, J. Am. Chem. Soc. 114 (1992) 8669.
[10] H. Ali, J.E. van Lier, Chem. Res. 99 (1999) 2379.
[11] B. Rodger, D. Naether, T. Lewald, M. Braune, C. Nowak, W. Freyer, Biophys. Chem. 35 (1990) 303.
[12] I. Rosenthal, C. Muraki-Krishna, P. Riesz, E. Ben-Hur, Radiation Res. 107 (1986) 136.
[13] W.S. Chan, J.F. Marschall, R. Svensen, J. Bedwell, I.A. Hart, Cancer Res. 50 (1990) 4533.
[14] C. Lavvoque, A. Pelegrin, J.E. van Lier, Br. J. Cancer 74 (1996) 1886.
[15] K. Kalka, N. Ahmad, T. Criswell, D. Boothman, H. Mukhtar, Cancer Res. 60 (2000) 5984.
[16] D. Leupold, W. Freyer, J. Photochem. Photobiol. B: Biol. 12 (1992) 311.
[17] D. Gust, T.A. Moore, A.L. Moore, S.J. Lee, E. Bittersmann, D.K. Luttrull, A.A. Rehms, J.M. DeGraziano, X.C. Ma, F. Gao, R.E. Belford, Science 248 (1990) 199.
[18] J. Janczak, R. Kubiak, Polyhedron 20 (2001) 2901.
[19] R.P. Linstead, J.M. Robertson, J. Chem. Soc. A (1936) 1736.
[20] S. Matsumoto, K. Matsuhama, J. Mizuguchi, Acta Crystallogr. C 55 (1999) 131.
[21] J. Janczak, Polish J. Chem. 74 (2000) 157.
[22] R. Kubiak, J. Janczak, K. Ejsmont, Chem. Phys. Lett. 245 (1995) 249.
[23] M.G. Cory, H. Hirose, M.C. Zerner, Inorg. Chem. 34 (1995) 2969.
[24] N. Ishikawa, D. Maurice, M. Head-Gordon, Chem. Phys. Lett. 260 (1996) 178.
[25] M.S. Liao, S. Scheiner, J. Chem. Phys. 114 (2001) 9780.
[26] A.M. Hor, R.O. Loutfy, Thin Solid Films 106 (1983) 291.
[27] H.G. Kubota, J. Muto, K.M. Itoh, J. Mater. Sci. Lett. 15 (1996) 1475.
[28] K.P. Krishankumer, C.S. Menon, J. Solid State Chem. 128 (1997) 27.
[29] A.T. Davidson, J. Chem. Phys. 77 (1982) 168.
[30] Y. Sakakibara, R.N. Bera, T. Mizutani, K. Ishida, M. Tokumoto, T. Tani, J. Phys. Chem. B 105 (2001) 1547.
[31] A. Endo, S. Matsumoto, J. Mizuguchi, J. Phys. Chem. A 103 (1999) 8193.
[32] S. Matsumoto, A. Endo, J. Mizuguchi, Z. Kristallogr. 215 (2000) 182.
[33] J. Mizuguchi, Z. Kristallogr. NCS 217 (2002) 1267.

[34] Enraf-Nonius, COLLECT, Nonius, Delft, The Netherlands, 1997–2000.
[35] Z. Otwinowski, W. Minor, in: C.W. Carter, Jr., R.M. Sweet (Eds.), Methods in Enzymology, vol. 276, Academic Press, New York, 1997, pp. 307–326.
[36] R.H. Blessing, Acta Crystallogr. A 51 (1995) 33.
[37] G.M. Sheldrick, SHELXS-97. Program for Crystal Structure Solution and Refinement, University of Göttingen, Göttingen, Germany, 1997.
[38] M.J. Frisch, G.W. Trucks, H.B. Schlegel, P.M.W. Gill, B.G. Johnson, M.A. Robb, J.R. Cheeseman, T. Keith, G.A. Petersen, J.A. Montgomery, K. Raghavachari, M.A. Al-Laham, V.G. Zakrzewski, J.V. Ortiz, J.B. Foresman, J. Cislowski, B.B. Stefanov, A. Nanayakkara, M. Challacombe, C.Y. Peng, P.Y. Ayala, W. Chen, M.W. Wong, J.L. Anders, E.S. Replogle, R. Gomperts, R.L. Martin, D.J. Fox, J.S. Binkley, D.J. Defrees, J. Baker, J.P. Stewart, M. Head-Gordon, C. Gonzalez, J.A Pople, GAUSSIAN94, Revision D.4, Gaussinan Inc., Pittsburgh, PA, 1995.
[39] J. Janczak, R. Kubiak, Polyhedron 21 (2002) 265.
[40] M.S. Fischer, D.H. Tempelton, A. Zalkin, M. Calvin, J. Am. Chem. Soc. 93 (1977) 2622.
[41] J. Mizuguchui, M. Mochizuki, Z. Kristallogr. NCS 217 (2002) 1267.
[42] R. Timkovich, A. Tulinsky, J. Am. Chem. Soc. 91 (1969) 4430.
[43] V. McKee, G.A. Rodley, Inorg. Chim. Acta 151 (1988) 233.
[44] S. Yang, R.A. Jacobson, Inorg. Chim. Acta 190 (1991) 129.
[45] H.Ch. Chow, R. Serin, Ch.E. Strouse, J. Am. Chem. Soc. 97 (1975) 7230.
[46] C. Kratky, J.D. Dunitz, Acta Crystallogr. B 33 (1977) 545.
[47] J. Mizuguchi, J. Phys. Chem. A 105 (2001) 10719.
[48] L. Pauling, The Nature of the Chemical Bond, 3rd edition, Cornell University Press, Ithaca, 1960, p. 262.
[49] R.J. Gillespie, J. Chem. Educ. 40 (1963) 295.
[50] R.J. Gillespie, Chem. Soc. Res. 20 (1992) 59.
[51] A.N. Sidorov, P. Kotlyar, Opt. Spectrosc. 11 (1961) 175.
[52] F.X. Sauvage, M.G. DeBacker, B. Stymne, Spectrochim. Acta A 38 (1982) 803.
[53] B. Stymne, F.X. Sauvage, G. Wettermark, Spectrochim. Acta A 36 (1980) 397.
[54] H.F. Shurvell, L. Pinzutti, Can. J. Chem. 44 (1966) 125.
[55] T. Kobayashi, F. Kurokawa, N. Uyeda, E. Suito, Spectrochim. Acta A 26 (1970) 1305.
[56] A.N. Sidorov, A.N. Terenin, Opt. Spectrosc. 8 (1960) 254.
[57] A.N. Sidorov, A.N. Terenin, Opt. Spectrosc. 8 (1960) 482.
[58] J.J. Katz, G.L. Closs, F.C. Pennington, M.R. Thomas, H.H. Strain, J. Am. Chem. Soc. 85 (1963) 3801.
[59] B. Stymne, F.X. Sauvage, G. Wettermark, Spectrochim. Acta A 35 (1979) 1195.
[60] A.N. Sidorov, P. Kotlyar, Opt. Spectrosc. 11 (1961) 92.
[61] J. Janczak, Polish J. Chem. 72 (1998) 1871.
[62] J. Janczak, Polish J. Chem. 73 (1999) 437.
[63] T. Kobayashi, Spectrochim. Acta A 26 (1970) 1313.
[64] C. Clarisse, M.T. Riou, Inorg. Chim. Acta 130 (1987) 139.
[65] G. Terzian, B. Moubaraki, M. Mossoyan-Deneux, D. Benlian, Spectrochim. Acta A 45 (1989) 675.
[66] J. Tomkinson, Spectrochim. Acta A 48 (1992) 329.
[67] A. Henriksson, M. Sundbom, Theoret. Chim. Acta 27 (1972) 213.
[68] A. Henriksson, B. Roos, M. Sundbom, Theor. Chim. Acta 27 (1972) 303.
[69] J. Mizuguchi, G. Rihs, H.R. Karfunkel, J. Phys. Chem. 99 (1995) 16217.
[70] J. Mizuguchi, J. Phys. Chem. A 105 (2001) 1121.
[71] T. Saito, W. Sisk, T. Kobayashi, S. Suzuki, T. Iwayanagi, J. Phys. Chem. 97 (1993) 8026.
[72] H.S. Naleva, T. Saito, A. Kakuta, T. Iwyanagi, J. Phys. Chem. 97 (1993) 10515.
[73] T. Saito, Y. Iwakabe, T. Kobayashi, S. Suzuki, T. Iwyanagi, J. Phys. Chem. 97 (1994) 2726.
[74] T.H. Huang, J.H. Sharp, Chem. Phys. 65 (1982) 205.
[75] Y. Pan, X. Liao, Y. Wu, L. Chen, Y. Zhao, Y. Shen, F. Li, S. Shen, D. Huang, Thin Solid Films 324 (1998) 209.
[76] N. Nanai, M. Yudasaka, Y. Ohki, S. Uoshimura, Thin Solid Films 298 (1997) 83.
[77] R.E. Ziolo, C.H. Griffits, J.M. Troup, J. Chem. Soc., Dalton Trans. (1980) 2300.
[78] K. Yamada, H. Hoski, K. Ishikawa, H. Takeoze, A. Fukuda, A. Saiki, J. Cryst. Growth 160 (1996) 279.
[79] W. Hiller, J. Strähle, W. Kobel, H. Hanack, Z. Kristallogr. 159 (1982) 173.
[80] K. Oka, O. Okada, K. Nukada, Jpn. J. Appl. Phys. 31 (1992) 2181.